



A greener route to prepare PEBAX®1074 membranes for gas separation processes

Paloma Ortiz-Albo^a, Vítor D. Alves^b, Izumi Kumakiri^c, Joao Crespo^a, Luísa A. Neves^{a,*}

^a LAQV/ REQUIMTE, Department of Chemistry, NOVA School of Science and Technology, FCT NOVA, Universidade NOVA de Lisboa, 2829-516, Caparica, Portugal

^b LEAF—Linking Landscape, Environment, Agriculture and Food, Associated Laboratory TERRA, Instituto Superior de Agronomia, Universidade de Lisboa, Tapada da Ajuda, 1349-017, Lisboa, Portugal

^c Graduate School of Sciences and Technology for Innovation, Yamaguchi University, 7558611, Ube, Japan

ARTICLE INFO

Keywords:

Rhodiasolv®Polarclean
Green solvent
Gas separation
Polymeric membranes
Phase inversion

ABSTRACT

The solvent used in membrane fabrication is crucial for a potential industrial application, with a direct effect on its safety, environmental and economic impact. Thus, in the last years, the search for greener and safer solvents became of utmost importance aiming for a sustainable fabrication of highly performing membranes, since that also affects the final membrane morphology. Typically, solvent evaporation-based methods are used for the preparation of membranes for gas separation processes, such as dip-coating and spray coating methods. The advantage of this approach relies on the possibility of using greener non-toxic solvents, such as water and ethanol. However, an alternative route might involve the use of phase inversion methods. In this procedure, the selection of the solvent will play an even more important role, with an impact on the gas separation membrane properties. Small defects or structural changes will decisively alter the final membrane performance.

In this work, it is presented for the first time the alternative use of a non-toxic and eco-friendly solvent, Rhodiasolv®Polarclean, for the preparation of CO₂-selective PEBAX®-based membranes using a hybrid phase inversion method. This preliminary study evaluates the relationship between the fabrication protocol, with the resulting structural, thermal, and mechanical membrane properties for self-standing membranes. The gas separation performance was tested for different gases: H₂, N₂, O₂, CO₂ and CH₄. This analysis also includes a comparison with the commonly used, although strongly restricted and hazardous, solvent N-Methyl-2-Pyrrolidone (NMP).

1. Introduction

The design of sustainable membrane processes has become a crucial task determining the selection of membrane materials as well as their preparation methods, and their end-of-life and disposal. The growing trend of using less toxic and harmless solvents has had an important impact on the development of new polymeric membranes over the last decades [1]. At the same time, the selection of an adequate solvent plays a key role in the resulting structural and performance properties of the prepared membrane. Considering phase inversion fabrication methods, a suitable solvent will also depend on preparation factors such as polymer solubility, dope solution viscosity, and miscibility with the non-solvent [1–3].

The background for this work considers alternative membrane preparation protocols involving phase inversion methods. Among the

several possibilities for preparing membranes, phase separation fabrication methods can be classified as non-solvent induced phase separation (NIPS), temperature-induced phase separation (TIPS), vapor induced phase separation (VIPS), and solvent evaporation induced phase separation (EIPS) protocols [4]. However, the use of non-toxic solvents for gas separation processes is still scarce, being easier to find research works focused on the use of bio-polymers [2] as option to improve membrane sustainability.

In this work, a hybrid protocol was developed to fabricate polymeric membranes based on PEBAX® as polymer, Rhodiasolv®Polarclean as solvent, and water as non-solvent. Rhodiasolv®Polarclean (Solvay Novacare, France), composed of variable (85–95 %) amounts of methyl 5-(dimethylamino)-2-methyl-5-oxopentanoate (C₉H₁₇NO₃), has raised interest as potential low-hazard and environment-friendly solvent obtained as a by-product of the manufacturing process of Nylon 6-6 [3,5,

* Corresponding author.

E-mail address: luisa.neves@fct.unl.pt (L.A. Neves).

<https://doi.org/10.1016/j.memsci.2023.122346>

Received 7 November 2023; Received in revised form 12 December 2023; Accepted 14 December 2023

Available online 18 December 2023

0376-7388/© 2023 The Authors. Published by Elsevier B.V. This is an open access article under the CC BY-NC-ND license (<http://creativecommons.org/licenses/by-nc-nd/4.0/>).

6]. The term “green solvent” has been used when referring to Rhodiasolv®Polarclean due to its biodegradability, and eco-toxicological profile, with no particular risks to human health (no skin irritation or mutagenic effects) [7,8], especially when compared to traditional solvents. Its composition and physicochemical properties have been studied previously, being its viscosity critical for its utilization compared to other green and conventional solvents [5]. However, its high boiling point and capacity to solubilize different polymers have motivated its use in the fabrication of membranes in previous works using polysulfone [3], polyether sulfone [8,9], and poly(vinylidene fluoride) [7,10], among others [2]. To further analyze the feasibility of non-toxic solvents for membrane production, several factors such as the solvent production, solvent recovery and cost must be addressed [4,11]. Previous research work [9] investigated the economic feasibility of shifting from conventional solvents (such as DMF or NMP, 2-3 €/kg) to more expensive Rhodiasolv®Polarclean (estimated 8 €/kg) in an European regulatory framework. Solvent recovery is key in this scenario aiming process sustainability and reduction of the final membrane cost. Nevertheless, to fully address a sustainable membrane fabrication, the circular economy and zero-waste approach must be further investigated, including a deep analysis of the additional costs and potential alternatives for solvent recovery (e.g. using distillation [4]). In this work, Rhodiasolv®Polarclean was combined with a different type of polymer to test a new alternative approach in membrane fabrication.

To first address the solvent-polymer compatibility, Hansen Solubility parameters have been typically used to anticipate the potential of dissolving the polymer by different solvents. Table 1 gathers the Hansen Solubility parameters of Rhodiasolv®Polarclean compared to other popular although toxic solvents, such as N,N-Dimethylformamide (DMF), DMA and N-Methyl-2-Pyrrolidone (NMP), along with the reference hazard code of each one of them [2,7,12]. The potential affinity of solvent-polymer can be described with the closeness of Hansen Solubility parameters. However, Hansen Solubility parameters of the specific polymer grade selected for the study was not available in the literature and therefore, it is considered that novel solvents with similar parameters to known suitable solvents will potentially solubilize the same polymer.

On the other hand, PEBAX® is a commercially available poly ether-block-amide co-polymer from the family of thermoplastic elastomers. It also presents customized properties depending on its monomers, molecular weight, and hard/soft ratios [13]. Tunable polymer characteristics based on the polyamide (PA) and poly-ether oxide (PEO) blocks define its chain mobility, caused by PEO groups, or its crystallinity and mechanical strength, related to crystalline PA blocks.

The use of PEBAX® has been studied mainly for water applications and gas separation processes and, more particularly, for CO₂ separation processes, due to its intrinsic high CO₂ affinity, attributed to the ether

oxide (EO) units in the polymer. While PEBAX® membranes have been evaluated for different processes, different combinations of PEBAX® with other CO₂-selective materials have been discussed in the literature to specifically upgrade the membrane performance, such as the use of ionic liquids (ILs) and microporous materials, such as metal-organic frameworks (MOFs). However, one of the most versatile properties of PEBAX® materials has been their use to form thin-film composite membranes [13]. In this regard, most gas separation membranes have been focused on specific grades, such as PEBAX®1657 and PEBAX®2533 [13]. The most used preparation methods rely on the possibility of dissolving these polymers in water/ethanol or butanol solvents, being possible to use solvent evaporation methods. This property makes PEBAX® polymers interesting for fabrication methods such as dip-coating (with a solvent evaporation step) and spray coating. In a previous work [14], it was evaluated the preparation of PEBAX®3533 via phase inversion method using butanol as solvent to prepare thin-film composite membranes. The protocol consisted in combining a dip-coating step, followed by a solvent exchange. Several dope solutions concentration and coatings were evaluated, successfully obtaining a dense layer over a polysulfone support without including a gutter layer.

Some few works have also considered PEBAX®1074 [15–18] for CO₂ separation, with appealing selective properties in terms of gas and vapor permeabilities [17]. The possibility of preparing membranes with PEBAX®1074, taking advantage of its fast gelation process due to the length of PA12 chain [13], makes it appealing for other preparation methods such as phase inversion. Therefore, the preparation of PEBAX®1074-based membranes using polar solvents, make it suitable as base polymer for our study with Rhodiasolv®Polarclean.

Our interest in combining an organic solvent, such as Rhodiasolv®Polarclean, with in this type of procedures also relies on its relatively high viscosity [5] compared to other organic solvents. Polymeric solutions with the same polymer concentration, but higher viscosity, will favor the formation of a thin film layer, reducing the potential polymer pore inclusion in the support. However, this will not be addressed in this work.

This work aims to show the potential of an alternative preparation route of PEBAX®-based self-standing flat membranes with gas separation properties through the utilization of green solvent Rhodiasolv®Polarclean via a phase inversion protocol.

This study comprises the analysis of polymer concentration in the dope solution, membrane characterization in terms of chemical composition, thermal, structural, and mechanical properties, and gas separation performance, comparing Rhodiasolv®Polarclean to the traditional solvent NMP, considered a highly hazardous and toxic solvent with strong regulatory restrictions for defined industries (batteries, semiconductors, fibers, and pharmaceuticals), by the European Union [2,4,6,19]. Up to the authors' knowledge, PEBAX®1074 membranes prepared by the phase inversion method, utilizing Rhodiasolv®Polarclean are reported in this work for the first time.

2. Materials and methods

2.1. Materials

PEBAX® MV 1074 SA 01, designed here as PEBAX®1074, and Rhodiasolv®Polarclean were kindly supplied by Arkema (France) and Solvay Novacare (France), respectively. N-Methyl-2-Pyrrolidone (Sigma Aldrich, >99.9 %) was also used as solvent. Where relevant, the solvent label was simplified using the acronyms: RHODIASOLV®POLARCLEAN and NMP, respectively for Rhodiasolv®Polarclean and N-Methyl-2-Pyrrolidone. The gases, N₂ (purity grade 99.99 %), O₂ (99.999 %), CH₄ (99.5 %), H₂ (>99.99 %), and CO₂ (99.998 %) were obtained from Praxair (Portugal).

Table 1

Hansen solubility parameters [2,8] and Hazard codes according to the European Regulation (EC) No. 1272/2008 [2,7,12] of Rhodiasolv®Polarclean compared to other conventional solvents: DMF, DMA, and NMP.

Solvent	δ_h (MPa) ^{0.5}	δ_d (MPa) ^{0.5}	δ_p (MPa) ^{0.5}	δ_t^a (MPa) ^{0.5}	Hazard codes
Rhodiasolv®Polarclean	9.2	15.8	10.7	21.2	H319
DMF	11.3	17.4	13.7	24.9	H226, H312, H332,H319
DMA	11.8	17.8	14.1	25.6	H360D, H312, H332
NMP	7.2	18.4	12.3	23.3	H315, H319, H335

^a $\delta_t = \sqrt{\delta_h^2 + \delta_d^2 + \delta_p^2}$; representing δ_h , the hydrogen bonding; δ_d , the dispersive force; and δ_p , the polar force.

2.2. Membrane preparation

PEBAX®1074 pellets were dissolved in Rhodiasolv®Polarclean with 11, 16, and 20 wt% of polymer concentration and in NMP with 16, 20, and 25 wt%. These concentrations were adapted depending on the viscosity of the dope solution, as Rhodiasolv®Polarclean presents a high viscosity (9 mPa s at 20 °C) compared to NMP (1.67 mPa s at 20 °C) [5]. Fig. 1 schematically represents the protocol herein described, as the embedded images of the gel-like structure obtained prior to the phase inversion (Fig. 1c), and the resulting membrane (Fig. 1e).

The polymer was successfully dissolved at 100 °C after 1 h and kept stirring to 130 °C for 2 h for complete moisture removal and degasification. The initially clear, slightly yellow solution turned into a light orange color. Dope solutions were cast in a glass plate as support and a manual casting knife (Elcometer 3580 Casting Knife, Elcometer, E.U.) with a gap of 50 µm. The casting of the membranes was performed at room conditions without any control. The temperature and relative humidity were monitored: 23 ± 2 °C, and with an average relative humidity of 55 %. The casted membranes were immersed in distilled water at approximately 20 °C for 30 min, and then cooled for 1 min at room temperature and washed with running 70 % ethanol in water. Finally, they were dried at 40 °C for 12 h.

2.3. Characterization techniques

Scanning Electron Microscopy (SEM) cross-section, top and bottom membrane surfaces images were obtained using a JEOL scanning electron microscope, model 7001F (USA) with an electron beam intensity of 20 kV. The samples neat cross-sections were cut by immersing the membranes in liquid nitrogen and Au–Pd was deposited prior to the acquisition of the images.

A Fourier Transform Infrared (FT-IR) Spectrometer Spectrum Two model (PerkinElmer, Spain) with an Attenuated Total Reflectance (ATR) modulus was used to obtain the spectra of solvent Rhodiasolv®Polarclean, prepared dope solutions of Rhodiasolv®Polarclean with dissolved PEBAX®1074, and PEBAX®1074-based membranes. Measurements were performed at room temperature conditions, between 4000 and 400 cm^{-1} , with a spectral resolution of 4 cm^{-1} .

An Elemental analyzer Flash EA 1112 CHNS series (Thermo Finnigan, Italy) was used to determine the elemental composition of the prepared membranes.

A Thermogravimetric Analyzer Setaram Labsys EVO (TGA, France) was utilized for thermal characterization of structural decomposition of

prepared gels of Rhodiasolv®Polarclean with dissolved PEBAX® MV 1074, and PEBAX®1074-based membranes. The maximum temperature, heating ramp and gas used were 500 °C, 10 °C/min and argon, respectively.

Differential Scanning Calorimetry (DSC 131, France) was utilized for the characterization of dope solutions. The analysis was performed with initial degasification of the sample *in situ* at 80 °C, followed by two cycles from room temperature to 150 °C, with a heating and cooling rate equal to 10 °C/min.

X-ray diffraction (XRD, PANalytical's X'Pert PRO diffractometer (Malvern Panalytical, UK) patterns of prepared membranes were obtained using Cu radiation with an X-ray generator of 40 kV voltage with 35 mA current. Patterns were collected in the 2θ range between 5° and 40° with a scanning speed of $(2\theta)/\text{min}$ and step width of $^\circ.0033$. Crystallinity and d -spacing parameters were calculated using Eq. (1) and Bragg's equation, Eq. (2):

$$\chi_c (\%) = 100 - \frac{100}{1 + \frac{\chi_c}{\chi_a}} \quad (\text{Eq. 1})$$

$$n\lambda = 2d \sin \theta \quad (\text{Eq. 2})$$

where χ_c and χ_a are the areas of the crystalline and amorphous regions from the XRD patterns, respectively, and n is a positive integer, λ the wavelength, and θ the angle of incidence.

Rheological studies of the Rhodiasolv®Polarclean-based dope solutions were performed using a rheometer Haake Mars™ III (Thermo Scientific, Germany) with a corrugated plate-plate geometry with 2 cm of diameter. The viscoelastic properties were analyzed by simulating the precipitation step after membrane casting, performing a temperature sweep from 125 °C to 90 °C at 2 °C/min, with a constant frequency of 1 Hz and constant tension (1.5 Pa). To analyze the effect of ambient relative humidity, additional tests were performed: cooling from 125 °C to 90 °C, followed by heating from 90 °C to 125 °C, and a time sweep at 130 °C for 20 min. In all tests, the dope solutions were previously heated at 130 °C for 30 min sealed from ambient atmosphere, prior to their transference into the rheometer. In each measurement, the elastic (G') and viscous (G'') moduli were measured as a function of temperature or time. Tensile tests were performed using a TA XT Plus Texture Analyzer (Stable Micro Systems, UK) at ambient temperature and relative humidity. Rectangular membrane strips (40 × 10 mm) were fixed to tensile grips and stretched at 1 mm/s. Tensile strength (stress) at break was calculated by the ratio between the force at break and the initial strip cross-section area. Elongation (strain) at break was calculated by dividing the sample length at the break by its initial length. Young modulus was obtained from the slope of the stress-strain curve in the elastic region. Three replicas were performed for each type of membrane.

Membrane swelling due to water absorption and water uptake was analyzed for all the prepared samples. The procedure consisted on the preparation of membranes with known area, thickness, and weight, followed by their total immersion in distilled water for 24 h at 30 °C, followed by drying of samples at 40 °C for 24 h. Membrane area, thickness, and weight were measured after smooth removal of superficial water, and after posterior drying. Membrane swelling was determined twice: from as-prepared conditions to post-immersion in water; and from post-immersion to dried state. Therefore, the structural stability and recovery after swelling were also addressed. The volumetric swelling of the membranes was estimated using differences in the membrane thickness (Eq. (3)), as membrane area changes were negligible, and the water uptake (Eq. (4)), from the differences in the membrane mass.

$$\text{Swelling} (\%) = \left(\frac{l_{\text{wet}} - l_i}{l_i} \right) \times 100 \quad (\text{Eq. 3})$$

where l_{wet} is the wet membrane thickness, and l_i is the thickness of the

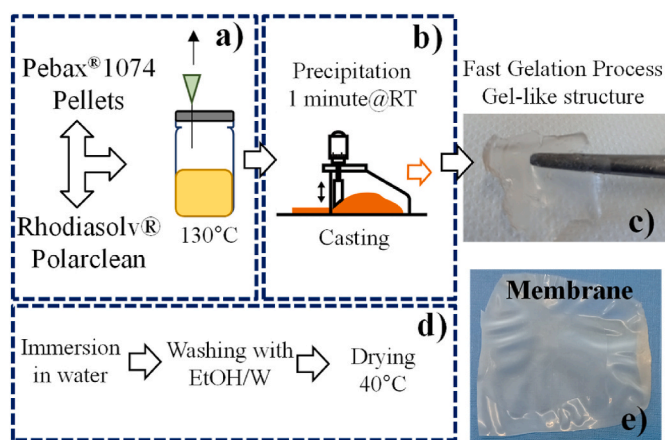


Fig. 1. Schematic representation of PEBAX®1074 fabrication protocol: a) preparation of dope solution; b) casting and precipitation steps; c) example of gel-like structure obtained from fast gelation process; d) phase inversion, solvent (water), and non-solvent removal (Ethanol/water); and e) example of obtained membrane.

dried membrane.

$$\text{Water uptake (g/g}_{\text{membrane}}) = \left(\frac{m_{\text{wet}} - m_i}{m} \right) \times 100 \quad (\text{Eq. 4})$$

where m_{wet} is the wet membrane mass, and m_i is the mass of the dried membrane.

A Drop Shape Analyzer (DSA 25B, Kruss GmbH, Germany) was used to perform the required static contact angle measurements by the sessile drop method. The selected fluid was distilled water at monitored room temperature conditions (21 ± 1 °C). The membranes were previously dried at 40 °C overnight.

2.3.1. Gas permeation

Pure gas permeability was obtained from constant volume-pressure decay permeation experiments, previously designed [20,21], consisting of a gas cell divided into two compartments of the same volume, separated uniquely by the membrane. Decay of feed pressure and increase of permeate pressure were monitored along time, and gas membrane permeability was calculated using Eq. (5).

$$P \cdot \frac{t}{l} = \frac{1}{\beta} \ln \left(\frac{\Delta p_0}{\Delta p} \right) \quad (\text{Eq. 5})$$

where P , is the pure gas membrane permeability (m^2/s), t , time (s), p , pressure (bar); l , membrane thickness (m); and β the experimentally determined system volumetric parameter, ($1/\text{m}$). The pure gases tested were H_2 , N_2 , O_2 , CH_4 , and CO_2 at 30 °C and 0.7 bar as driving force. Pure gas membrane permeability was converted to barrer units as: 1 barrer = $10^{-10} \text{ cm}^3_{\text{TP}} \cdot \text{cm}/\text{cm}^2/\text{s} \cdot \text{cmHg}^{-1} = 8.3 \cdot 10^{-13} \text{ m}^2/\text{s}$ [22]. Ideal selectivity of gas i over j was calculated as the ratio of permeability coefficients:

$$\alpha_{ij} = \frac{P_i}{P_j} \quad (\text{Eq. 6})$$

2.4. Simulation study

Linear and volumetric molecule size of Rhodiasolv®Polarclean (methyl 5-(dimethylamino)-2-methyl-5-oxopentanoate), NMP, and water were estimated using Materials Studio version 8 supplied by BIOSYM Inc. The molecules were designed (Fig. S1 in the Supporting Information) and the Universal Force Field (UFF) was selected to prepare a cubic cell with 10 Å of lattice occupied by one molecule of solvent at 298 K. The molecules were energetically and structurally optimized using an NVT (constant number of molecules, volume, and temperature) dynamic simulation for 200 ps at 298 K. Fractional free volume (FFV) was used to determine the volumetric size of the molecule considering a Connolly radius of 1 Å. Molecule size was considered as the occupied volume inside the cell.

3. Results and discussion

3.1. Dope solution characterization

Dope solutions were prepared by dissolving the designed polymer amount in Rhodiasolv®Polarclean. Samples from the dope solutions were taken for characterization by FT-IR. At room temperature, the dope solution is in a gel-like state due to the high hygroscopic behavior of the sample. Additionally, Rhodiasolv®Polarclean-based dope solutions were characterized through DSC analysis to determine the transition temperatures (Table 2).

Fig. S2 gathers the normalized spectra of Rhodiasolv®Polarclean solvent and a PEBAX® 1074 membrane prepared from a dope solution of 16 wt% of polymer. The composition from both polymer and solvent are effectively identified and correspond to previously reported data [5, 23–26].

Rhodiasolv®Polarclean is composed of methyl 5-(dimethylamine)-2-

Table 2

Transition temperatures for Rhodiasolv®Polarclean and structures composed by 11, 16 and 20 wt% PEBAX®1074 dissolved in Rhodiasolv®Polarclean from the second temperature cycle.

Polymer (wt.%)		11	16	20
Melting	T_{onset} (°C)	90	105	98
	T_{offset} (°C)	132	131	134
Crystallization	T_{onset} (°C)	117	119	120
	T_{offset} (°C)	68	78	77

methyl-5-oxopentanoate ($\text{C}_9\text{H}_{17}\text{N}_1\text{O}_3$). Water was identified through the bonds of –OH at 3500 cm^{-1} . In the region of 3000 cm^{-1} , aliphatic C–H bonds can be ascribed in both solvent and membrane. A characteristic double peak from the polymer was identified in this region, along with the peak at 3308 cm^{-1} , associated with N–H groups in the PA segment.

The peak at 1120 cm^{-1} of the pure PEBAX® 1074 membrane relates to the symmetric vibration of the C–O–C group in the PEO segment. Peaks at 1646 cm^{-1} and 1734 cm^{-1} are related to H–N–C=O and O–C=O groups in the PA segment, respectively, while the aliphatic C–H bond is assigned by the peaks in the region $2800\text{--}3000 \text{ cm}^{-1}$. The peak at 3308 cm^{-1} is associated with N–H groups in the PA segment, C–H aliphatic at 2922 cm^{-1} , C–O–C from the PEO group, and H–N–C=O group from PA fragment.

The fabrication protocol was analyzed using rheology studies (viscoelastic properties) upon induction of the precipitation step during preparation (Fig. 1b), considering that the effects of cooling and precipitation rate depend from the starting dope solution. The effect of the dope solution composition and temperature on the solution rheology is characterized by the elastic or storage (G') and viscous or loss (G'') moduli, presented in Fig. 2. The small strain oscillatory tests with low cooling rates were performed to detect the “gel point”, the temperature at which the storage modulus (G') crosses the loss modulus (G'') [27]. The gel point was only possible to be perceived for the lowest polymer concentration (11 wt%) at the highest temperature tested. For higher polymer concentrations (16 and 20 wt%), G' was larger G'' over the entire temperature range studied. This fact is attributed to the larger number of molecules present enabling the polymeric network formation even at the highest temperature studied. In addition, particularly for 11 and 16 wt% concentrations, a reinforcement of the polymeric structures may be observed upon cooling, as there is an increase of both moduli values, along with an increase of G' over G'' .

Further rheology tests were performed, and the results were included in the Supporting Information (Figs. S3a–c). As consequence of the tests

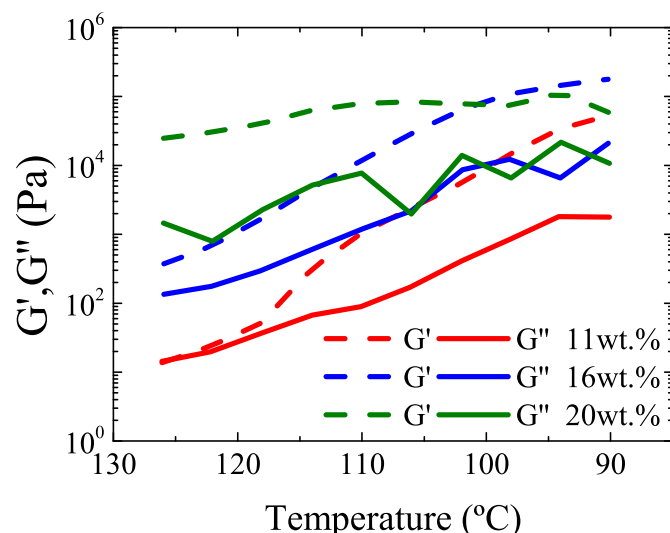


Fig. 2. Cooling effect on viscoelastic properties of dope solutions for different polymer concentrations.

being carried out in an open atmosphere, the contact to ambient relative humidity (20 °C and 45%RH) over time is envisaged to affect the viscoelastic properties. As such, these properties were additionally studied in three consecutive steps, analysing the dynamic moduli when cooling from 125 °C to 90 °C, followed by heating from 90 °C to 125 °C, and then kept at 130 °C for 20 min. It may be observed that the values of dynamic moduli after the three steps are higher than their initial value, for all polymer concentrations studied, even though a similar temperature was reached at the end. This fact indicates that the gel structure is not the same, which might be due to the effect of water vapor absorption.

An additional test was performed using the polymer concentration of 11 wt%, consisting of a time sweep at a constant temperature of 130 °C (Fig. S3d). The results show that both moduli increase over time, indicating that the atmospheric water vapor in contact with the sample is changing its viscoelastic properties.

In contrast to the rheological studies, the DSC results were obtained under an inert atmosphere. Two phenomena were observed: a melting process while heating the sample and crystallization in the cooling. Higher polymer concentrations required a higher temperature to start melting. Therefore, the membrane formation depended strongly on the precipitation step, influenced by both the temperature and the relative humidity.

3.2. Chemical and structural characterization

Self-standing PEBAX®1074 membranes were successfully prepared for 11, 16 and 20 wt% in the dope solution using Rhodiasolv®Polarclean, and 16, 20 and 25 wt% using N-Methyl-2-Pyrrolidone. Elemental Analysis results (Table 3) are useful for polymer composition estimation. Standard deviation was obtained from analytical replicas being below ± 0.7 . Bondar et al. [28] characterized PEBAX®1074, obtaining mass percentages similar to the prepared membranes: N – 3.23 %; C – 62.03 %; H – 11.00 %. Following their methodology, the amount of PEO segments was estimated to be around 54 % for all prepared membranes, which is in good agreement with the value reported in the literature (55 %) [13,28]. Therefore, the chemical composition of the membranes was not affected by the new preparation method. The chemical composition variations of the final polymer, resulting from different preparation conditions, negligible. Fig. S4 in the Supporting Information shows the XRD patterns from the prepared membranes, from which the crystallinity percentage and *d*-spacing were estimated and included in Table 3. Three main diffraction peaks were identified in the semi-crystalline polymer: 22.6° and 5.6° (2 θ), corresponding to (001) and (020) γ form of crystal from PA diffractions, and at 11.3° (2 θ), related to the PEO regions [25]. As previously mentioned, solvent selection has a crucial effect on the final membrane properties [21]. Membranes prepared with NMP as solvent resulted in more crystalline membranes, and higher starting polymer concentration led to higher crystallinity percentage [13], achieving an apparent plateau near 50 %. Comparing both solvents, NMP has a lower solubility in water (≥ 100 g/L at 20 °C [29]) than Rhodiasolv®Polarclean (≥ 490 g/L at 24 °C [5]), which potentially slows down the polymer chain arrangement during its exchange with the non-solvent water during the phase inversion step, leading to a more

crystalline polymeric structure after drying. Additionally, the solvent molecule sizes were estimated using molecular simulations for Rhodiasolv®Polarclean and NMP (Fig. S1 and Table S1 in Supporting Information). Rhodiasolv®Polarclean, simplified as methyl 5-(dimethylamino)-2-methyl-5-oxopentanoate, presented a three times larger linear size, and close to double in volumetric size and surface area. All these molecular-level differences between both solvents will affect the exchange with the small water molecules, leading to a different free volume between the polymeric chains.

The *d*-spacing was also determined for all prepared membranes (Table 3). PA (001) corresponds to the peak with higher intensity for all membranes and shows an increasing value with increasing crystallinity percent. This feature can be related to a higher distance between polymer chains and therefore, fewer interactions [21]. On the other hand, membranes prepared with Rhodiasolv®Polarclean presented the opposite trend for PA (020) and PEO, regardless of the increasing concentration and global crystalline behavior.

Fig. 3 shows the normalized FT-IR spectra of membranes prepared with different polymer concentrations in the dope solutions using Rhodiasolv®Polarclean and N-Methyl-2-Pyrrolidone, highlighting two specific wavenumber ranges: from 3000 to 2800 cm^{-1} (Fig. 3a) and from 1200 to 700 cm^{-1} (Fig. 3b). The complete spectra from 4000 to 400 cm^{-1} were included in Fig. S5, in Supporting Information. All membranes successfully confirmed the characteristic spectra of PEBAX®1074 without apparent solvent-associated peaks, as discussed in Section 3.1 [24–26]. In general terms, there were no significant variations between solvents, although some specific peaks suffered absorbance variations. In the highlighted ranges, C–H stretching aliphatic bonds in Fig. 3a and C–H bending bonds and Fig. 3b shows an opposite absorbance change depending on the membrane tested. Relating these observations to the crystallinity results from Table 2, lower crystallinity values show an increasing trend in absorbance values of C–H stretching aliphatic bonds, while C–H bending bonds decrease with lower crystallinity values. Therefore, the mobility capacity of the polymeric chains is affected by the fabrication method (solvent and polymer concentration) although negligible changes are observed in the overall membrane composition.

Fig. S6 gathers the SEM images of the prepared membranes with different solvents and starting polymer concentrations. The top, bottom and cross-section surfaces were analyzed for each case. Dense membranes with no apparent voids or defects were obtained, with important apparent rugosity differences between the top membrane surface, that is, the surface in contact with the atmosphere during the preparation, and the bottom surface, which was in contact with the glass substrate in the casting.

3.3. Thermal, mechanical and swelling properties

Fig. 4 shows the mass weight loss and derivative weight loss of as-prepared membranes up to 500 °C. Mass decay was not relevant in the range of room temperature to 100–150 °C, and therefore, it may be assumed that water (b.p. 100 °C) and ethanol (b.p. 78 °C) were effectively removed during the drying step. Two mass declines were identified: a smooth decrease, initiating at 150–175 °C; and the main decomposition decay, starting from 300 °C.

Table 3

Membrane composition determined by elemental analysis (standard deviation below ± 0.7) for the different solvents used and polymer concentration in dope solution.

Membrane	Elemental Analysis (wt.%)			PEO (wt.%)	<i>d</i> -spacing (Å)			Crystallinity (%)
	N	C	H		PA (020)	PEO	PA (001)	
11 wt%-PC	3.3	60.1	9.9	54.0 \pm 0.5	15.4	7.7	4.0	15.8
16 wt%-PC	3.4	60.6	9.6	52.1 \pm 0.4	15.2	7.6	4.1	36.9
20 wt%-PC	3.4	61.7	10.3	52.9 \pm 0.6	15.1	6.8	4.1	39.7
16 wt%-NMP	3.3	61.5	10.4	53.4 \pm 0.7	15.4	7.1	4.1	44.8
20 wt%-NMP	3.2	60.5	10.4	54.7 \pm 0.3	17.1	7.5	4.1	51.1
25 wt%-NMP	3.2	61.7	10.3	55.7 \pm 0.3	17.1	7.2	4.1	49.6

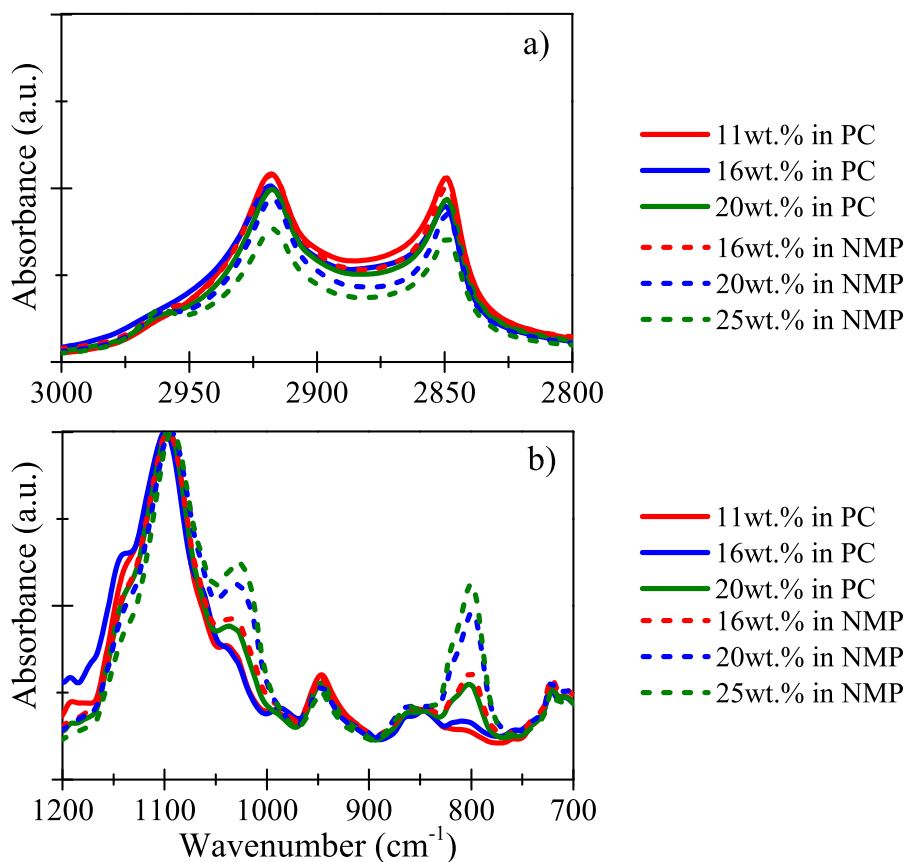


Fig. 3. FT-IR spectra in a) 3000 to 2800 cm^{-1} range and b) 1200 to 700 cm^{-1} of prepared membranes considering different polymer concentrations and solvents Rhodiasolv®Polarclean (PC) and N-Methyl-2-Pyrrolidone (NMP).

The first decrease of weight mass was not observed for every membrane in the same magnitude, being always below 10 wt%, observed from 150 °C. As the melting temperature of the polyamide block occurs at 156 °C, and the polymer melts at 158 °C according to other works [15], this decrease could be potentially associated with degradation and polymerization that increase the crystalline percentage (Table 2). On the other hand, the most significant, and common in all cases, membrane weight loss was observed from 300 °C, with the highest decomposition decay around 400–425 °C. The remains of the membranes at 500 °C were below 10 wt% of the initial mass. These decays were effectively associated with other PEBAX®1074-based membranes prepared by other methods in previous works [18,23,26].

Table 4 gathers the average membrane thickness, Young modulus, tensile strength, and elongation at break obtained from tensile experiments for the prepared membranes. As an exception, the membrane prepared with 25 wt% of polymer using NMP as solvent was not possible to break, under the conditions tested with the equipment described.

Considering the calculated average values, the membranes prepared with higher starting polymer concentration show higher Young modulus and tensile strength, which allowed for higher elongation before breaking. Though the membranes prepared with NMP presented similar Young modulus' values when compared to those produced with Rhodiasolv®Polarclean for the same polymer concentration, the tensile strength and elongation at break tended to be higher for membranes prepared with NMP. Comparing these observations to the membrane structural properties, it is possible to directly relate the membrane crystallinity with the mechanical properties (Table 3). Membranes prepared with NMP presented a higher crystalline degree, which translates into higher mechanically resistant structures, within the limit of the elastomer PEBAX®1074.

Additionally, membrane swelling and water uptake after immersion

in water for 24 h was determined (Table 4). Among the membranes produced with the same solvent, the highest polymer concentration resulted in the lowest swelling degree. This fact is attributed to the formation of a denser polymeric network with increasing polymer concentration, leading to lower water absorption. When comparing membranes produced with the same polymer concentration, but different solvents, higher swelling degree values were observed for the membranes produced with Rhodiasolv®Polarclean. The trend of the water uptake was not as linear as swelling values showing high standard deviation, especially for those prepared with NMP, which presented higher crystallinity degree. On the other hand, membranes prepared with Rhodiasolv®Polarclean showed higher water uptake with lower polymer concentration in the dope solution, coinciding with the higher swelling degree and lower crystallinity degree. Fig. S7 in the Supporting Information includes the images of the contact angle for Pebax®1074 membranes prepared with 16 wt% of polymer in the dope solution. The variation on the contact angle values did not provide relevant information, but it was possible to observe during the sessile drop analyses, the swelling of the membranes.

3.4. Gas permeation

Pure gas permeation studies were performed for the prepared membranes at 0.7 bar and 30 °C. Fig. 5 gathers the calculated pure gas permeability coefficients against the tested Lennard-Jones diameters [20,30–32] for H_2 (2.83 Å), O_2 (3.47 Å), CH_4 (3.76 Å), N_2 (3.80 Å), and CO_2 (3.94 Å). Averaged permeability values with standard deviation were calculated from independently prepared membrane replicas.

Fig. 6a compares the CO_2 permeability to the estimated membrane crystallinity percentage (Table 2), and Fig. 6b shows the ideal selectivity CO_2/N_2 against CO_2 permeability, compared to the Robeson upper

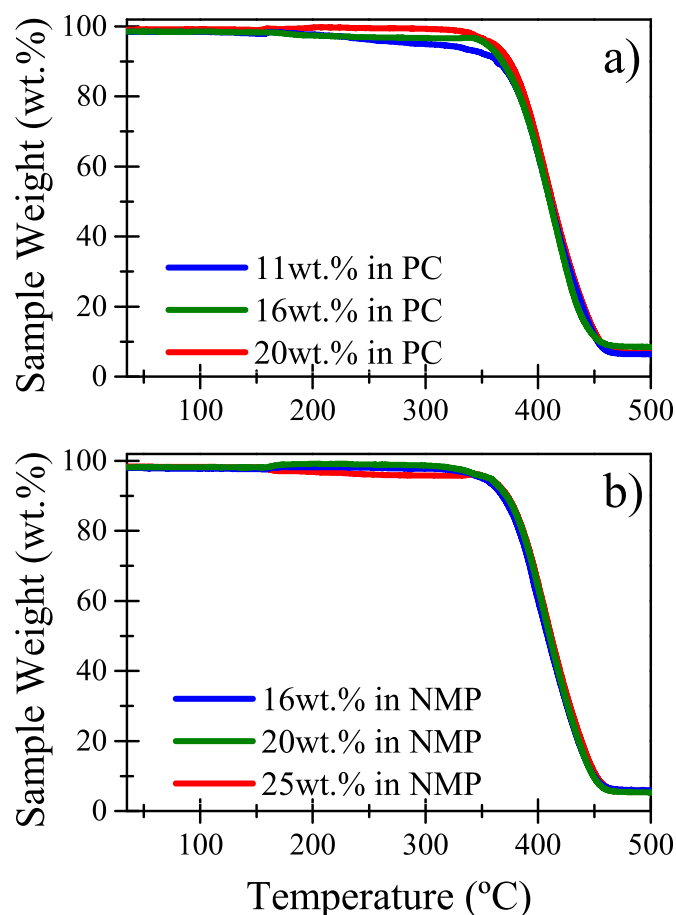


Fig. 4. Mass loss as a function of temperature for prepared membranes using a) Rhodiasolv®Polarclean (PC) and b) N-Methyl-2-Pyrrolidone (NMP) considering different polymer concentrations at the dope solution.

bound [33,34] and other works in the literature using Pebax®1074 as polymer [13,15,36–38].

The prepared membranes presented higher permeability towards CO₂ over the other tested gases, with N₂ showing the lowest permeability. In general terms, a higher polymer concentration in the dope solution leads to lower gas permeabilities. The unique exception was H₂ for membranes prepared with Rhodiasolv®Polarclean. These differences in the general trend have also been found in other membrane parameters, such as d-spacing for PEO and PA (020), and estimated PEO percent (Table 3), being potentially caused by the interactions of polymer with the solvent. Comparing the structural properties of the prepared membranes, it was possible to relate the membrane-determined crystallinity (Table 3) with the CO₂ membrane permeability (Fig. 6a) showing a general decreasing gas permeability with increasing crystallinity percentage. As the gas permeability is affected by the motion of the polymeric chain, a higher restriction of polymer movement leads to lower

gas permeability, as crystalline segments are considered to be more rigid [25]. At higher concentrations and for membranes prepared with NMP, the trend became less significant, achieving an apparent plateau of crystallinity-CO₂ permeability.

Comparing the most optimal separation, that is, CO₂/N₂ ideal selectivity against CO₂ permeability (Fig. 6b), all prepared membranes were below the Robeson upper bound of 2008 and comparable to other preparation approaches, which was something expectable for a pure conventional polymeric membrane. However, comparing the different parameters on the preparation route, it can be concluded that membranes prepared with Rhodiasolv®Polarclean present a higher separation performance, being more permeable for lower polymer concentration in the dope solution (11 wt%). It was also found an optimal balance between CO₂ permeability and CO₂/N₂ ideal selectivity for membranes prepared with 16 wt% using Rhodiasolv®Polarclean. Membrane permeability, typically expressed in barrer, is equal to the product of membrane permeance and membrane thickness. Higher membrane permeance values will be obtained for thinner membranes. Industrial applications for CO₂ separation consider commercially available polymeric membranes with high CO₂ permeance (higher than 1000 GPU) and CO₂/N₂ selectivity values over 40 [35]. Therefore, while PEBA[®] based membranes prepared with Rhodiasolv®Polarclean show appealing separation selectivities, the membrane preparation process must be optimized in order to obtain thinner selective membranes, and consequently higher CO₂ permeation performance.

4. Conclusions

The non-toxic Rhodiasolv®Polarclean solvent was successfully utilized for the fabrication of elastomer PEBA[®]1074-based membranes with gas separation properties. The fabrication protocol consisted of a hybrid phase inversion method TIPS/VIPS/NIPS. The temperature and ambient relative humidity contributed to the fast gelation process of the polymer before solvent removal with water as non-solvent. The prepared membranes presented a similar composition to the ones commonly obtained with the hazardous solvent NMP. The structural characteristic with higher impact in the membrane properties was the polymer semicrystalline structure. Membranes prepared with Rhodiasolv®Polarclean present a lower crystallinity, which led to lower tensile strength and higher CO₂ permeability. Therefore, the alternative use of the non-toxic solvent Rhodiasolv®Polarclean presents a high potential for preparing membranes with CO₂-selective behavior, following a more sustainable preparation route.

Associated content

Supporting Information: Figs. S1–S6 and Table S1.

Funding sources

The authors acknowledge “Fundação para a Ciência e Tecnologia” through the PhD grant SFRH/BD/139389/2018 (P. Ortiz-Albo). This work was also supported by the Associate Laboratory for Green

Table 4

Mechanical properties from tensile experiments, membrane swelling and water uptake values for membranes produced with different solvents and polymer concentrations (average ± standard deviation).

Membrane	Thickness (μm)	Young Module (10 [4] Pa)	Tensile Strength at break (10 [4] Pa)	Elongation at Break (–)	Swelling (%)	Water uptake (g/g membrane)
11 wt%-PC	42 ± 17	23 ± 5	1.6 ± 0.4	1.5 ± 1.2	51 ± 2	291 ± 15
16 wt%-PC	47 ± 6	27 ± 2	3.3 ± 0.5	2.5 ± 1.0	57 ± 6	185 ± 48
20 wt%-PC	121 ± 6	30 ± 8	6.1 ± 0.5	1.8 ± 0.9	30 ± 2	95 ± 26
16 wt%-NMP	46 ± 12	26 ± 5	3.7 ± 0.4	2.9 ± 1.6	28 ± 9	189 ± 28
20 wt%-NMP	141 ± 11	30 ± 12	8.5 ± 1.2	5.1 ± 1.2	19 ± 3	117 ± 30
25 wt%-NMP	146 ± 10	41 ± 10	>11 ^a	>12 ^a	18 ± 2	142 ± 26

^a The membrane break was not attained.

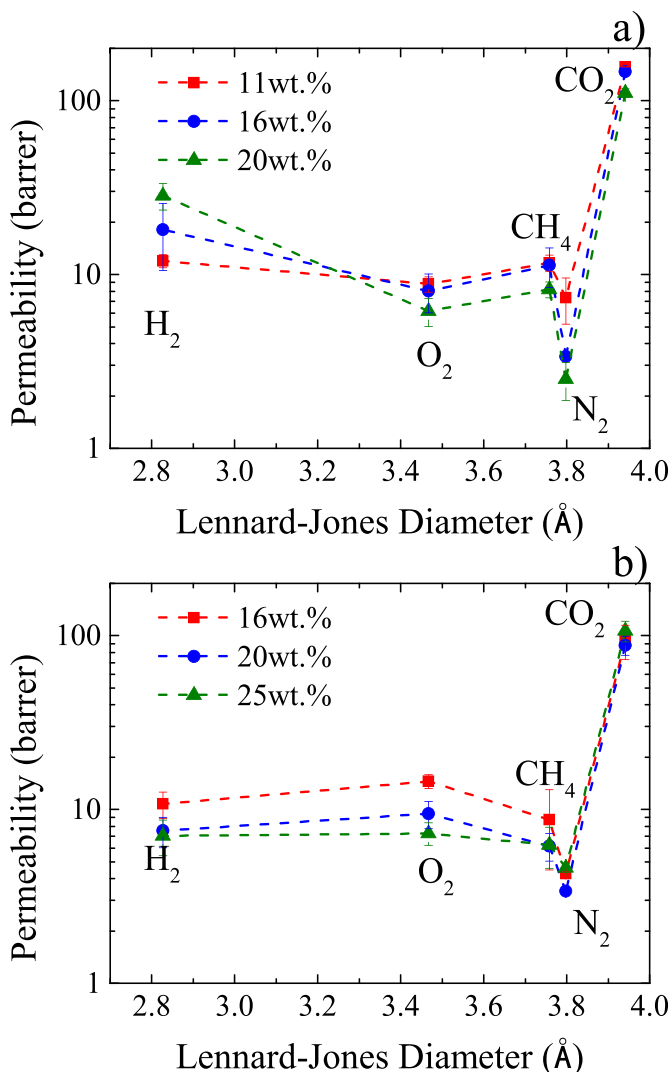


Fig. 5. Pure gas permeability values H₂ (2.83 Å), O₂ (3.47 Å), CH₄ (3.76 Å), N₂ (3.80 Å), and CO₂ (3.94 Å) for PEBAX®1074 membranes prepared with: a) Rhodiasolv® Polarclean and b) N-Methyl- 2-Pyrrolidone.

Chemistry- LAQV (Portugal) and LEAF—Linking Landscape, Environment, Agriculture and Food—Research Center, which are financed by national funds from FCT/MCTES (UIDB/50006/2020, UIDP/50006/2020 and UIDB/04129/2020) and for the research project PTDC/CTM-CTM/29869/2017 and Chugoku Regional Innovation Research Center, Japan.

Notes

There are no conflicts to declare.

CRedit authorship contribution statement

Paloma Ortiz-Albo: Conceptualization, Data curation, Investigation, Methodology, Writing – original draft. **Vítor D. Alves:** Investigation, Methodology, Writing – review & editing. **Izumi Kumakiri:** Supervision, Writing – review & editing. **Joao Crespo:** Supervision, Writing – review & editing. **Luísa A. Neves:** Conceptualization, Funding acquisition, Supervision, Writing – review & editing.

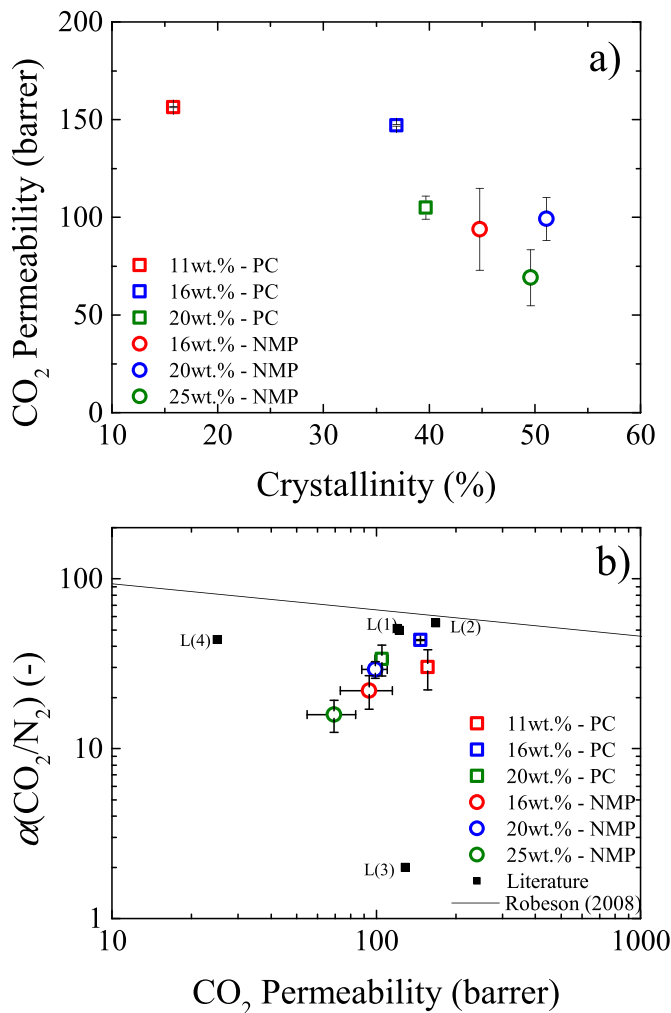


Fig. 6. Comparison of CO₂ permeability against a) estimated membrane crystallinity percentage, and b) ideal selectivity CO₂/N₂ compared to Robeson upper-bound (2008) and other PEBAX®1074 membranes prepared differently, such as by the solvent evaporation method L(1) - butanol and L(2) - propanol/water, L(3) - extruded film, and L(4) - solvent evaporation combined with washing with water using NMP as solvent [13,15,36–38].

Declaration of competing interest

The authors declare that they have no known competing financial interests or personal relationships that could have appeared to influence the work reported in this paper.

Data availability

Data will be made available on request.

Acknowledgment

The authors acknowledge “Fundação para a Ciência e Tecnologia” through the PhD grant SFRH/BD/139389/2018 (P. Ortiz-Albo). This work was also supported by the Associate Laboratory for Green Chemistry- LAQV (Portugal) and LEAF—Linking Landscape, Environment, Agriculture and Food—Research Center, which are financed by national funds from FCT/MCTES (UIDB/50006/2020, UIDP/50006/2020 and UIDB/04129/2020) and for the research project PTDC/CTM-CTM/29869/2017 and Chugoku Regional Innovation Research Center, Japan. Luísa A. Neves acknowledge Fundação para a Ciência e a Tecnologia (FCT)/MCTES) for the assistant researcher contract under Scientific

Employment Stimulus (2022.00689.CEECIND).

Appendix A. Supplementary data

Supplementary data to this article can be found online at <https://doi.org/10.1016/j.memsci.2023.122346>.

References

- [1] A. Figoli, T. Marino, S. Simone, E. Di Nicolò, X.-M. Li, T. He, S. Tornaghi, E. Drioli, Towards non-toxic solvents for membrane preparation: a review, *Green Chem.* 16 (9) (2014) 4034–4059, <https://doi.org/10.1039/C4GC00613E>.
- [2] D. Zou, S.P. Nunes, L.F.J. Vankelecom, A. Figoli, Y.M. Lee, Recent advances in polymer membranes employing non-toxic solvents and materials, *Green Chem.* 23 (24) (2021) 9815–9843, <https://doi.org/10.1039/D1GC03318B>.
- [3] X. Dong, H.D. Shannon, C. Parker, S. De Jesus, I.C. Escobar, Comparison of two low-hazard organic solvents as individual and cosolvents for the fabrication of polysulfone membranes, *AIChE J.* 66 (1) (2020), 16790.
- [4] X. Dong, D. Lu, T.A.L. Harris, I.C. Escobar, Polymers and solvents used in membrane fabrication: a review focusing on sustainable membrane development, *Membranes* 11 (5) (2021) 309, <https://doi.org/10.3390/MEMBRANES11050309>.
- [5] A. Randová, L. Bartovská, P. Morávek, P. Matějka, M. Novotná, S. Matějková, E. Drioli, A. Figoli, M. Lanč, K. Friess, A fundamental study of the physicochemical properties of Rhodiasolv® PolarClean: a promising alternative to common and hazardous solvents, *J. Mol. Liq.* 224 (2016) 1163–1171, <https://doi.org/10.1016/J.MOLLIQ.2016.10.085>.
- [6] N. Winterton, The green solvent: a critical perspective, *Clean Technol. Environ. Policy* 23 (9) (2021) 1, <https://doi.org/10.1007/S10098-021-02188-8>.
- [7] F. Russo, C. Ursino, B. Sayinli, I. Koyuncu, F. Galiano, A. Figoli, L. Aldieri, Advancements in sustainable PVDF copolymer membrane preparation using Rhodiasolv® PolarClean as an alternative eco-friendly solvent, *Cleanroom Technol.* 3 (4) (2021) 761–786, <https://doi.org/10.3390/CLEANTECHNOL3040045>, Pages 761–786 2021.
- [8] T. Marino, E. Blasi, S. Tornaghi, E. Di Nicolò, A. Figoli, Polyethersulfone membranes prepared with Rhodiasolv® PolarClean as water soluble green solvent, *J. Membr. Sci.* 549 (2018) 192–204, <https://doi.org/10.1016/j.memsci.2017.12.007>.
- [9] C. Ursino, F. Russo, R.M. Ferrari, M.P. De Santo, E. Di Nicolò, T. He, F. Galiano, A. Figoli, Polyethersulfone hollow fiber membranes prepared with PolarClean® as a more sustainable solvent, *J. Membr. Sci.* 608 (2020), 118216, <https://doi.org/10.1016/j.memsci.2020.118216>.
- [10] N.T. Hassankiadeh, Z. Cui, J.H. Kim, D.W. Shin, S.Y. Lee, A. Sanguineti, V. Arcella, Y.M. Lee, E. Drioli, Microporous poly(vinylidene fluoride) hollow fiber membranes fabricated with PolarClean as water-soluble green diluent and additives, *J. Membr. Sci.* 479 (2015) 204–212, <https://doi.org/10.1016/j.memsci.2015.01.031>.
- [11] S.P. Nunes, P.Z. Culfaz-Emecen, G.Z. Ramon, T. Visser, G.H. Koops, W. Jin, M. Ulbricht, Thinking the future of membranes: perspectives for advanced and new membrane materials and manufacturing processes, *J. Membr. Sci.* (2020), <https://doi.org/10.1016/j.memsci.2019.117761>.
- [12] D. Prat, A. Wells, J. Hayler, H. Sneddon, C.R. McElroy, S. Abou-Shehata, P.J. Dunn, CHEM21 selection guide of classical- and less classical-solvents, *Green Chem.* 18 (1) (2015) 288–296, <https://doi.org/10.1039/C5GC01008J>.
- [13] A. Selomon, L. Martínez-Izquierdo, M. Malankowska, C. Téllez, J. Coronas, Poly (Ether-Block-Amide) Copolymer Membranes in CO₂ Separation Applications, vol. 35, 2021, pp. 17085–17102, <https://doi.org/10.1021/acs.energyfuels.1c01638>.
- [14] L. Martínez-Izquierdo, M. Malankowska, C. Téllez, J. Coronas, Phase inversion method for the preparation of Pebax® 3533 thin film membranes for CO₂/N₂ separation, *J. Environ. Chem. Eng.* 9 (4) (2021), 105624, <https://doi.org/10.1016/J.JECE.2021.105624>.
- [15] Y. Shanguan, Intrinsic Properties of Poly(Ether-B-Amide) (Pebax® 1074) for Gas Permeation and Pervaporation, Master Thesis, Waterloo University, 2011.
- [16] N. Azizi, T. Mohammadi, R. Mosayebi Behbahani, Comparison of permeability performance of PEBAX-1074/TiO₂, PEBAX-1074/SiO₂ and PEBAX-1074/Al₂O₃ nanocomposite membranes for CO₂/CH₄ separation, *Chem. Eng. Res. Des.* 117 (2017) 177–189, <https://doi.org/10.1016/j.cherd.2016.10.018>.
- [17] J. Potreck, K. Nijmeijer, T. Kosinski, M. Wessling, Mixed water vapor/gas transport through the rubbery polymer PEBAX® 1074, *J. Membr. Sci.* 338 (1–2) (2009) 11–16, <https://doi.org/10.1016/j.memsci.2009.03.051>.
- [18] S. Azizi, N. Azizi, R. Homayoon, Experimental study of CO₂ and CH₄ permeability values through pebax-1074/silica mixed matrix membranes, *Silicon* 11 (2019) 2045–2057, <https://doi.org/10.1007/s12633-018-0021-z>.
- [19] D. Kim, S.P. Nunes, Green solvents for membrane manufacture: recent trends and perspectives, *Curr. Opin. Green Sustainable Chem.* 28 (2021), 100427, <https://doi.org/10.1016/J.COCS.2020.100427>.
- [20] L.A. Neves, J.G. Crespo, I.M. Coelho, Gas permeation studies in supported ionic liquid membranes, *J. Membr. Sci.* 357 (1–2) (2010) 160–170, <https://doi.org/10.1016/j.memsci.2010.04.016>.
- [21] M. Isanejad, N. Azizi, T. Mohammadi, Pebax membrane for CO₂/CH₄ separation: effects of various solvents on morphology and performance, *J. Appl. Polym. Sci.* 134 (9) (2017), 44531.
- [22] E.L. Cussler, Diffusion: Mass Transfer in Fluid Systems, second ed., Cambridge University Press, 2009.
- [23] W. Li, Z. Chang, L. Lin, X. Xu, Effect of montmorillonite on PEBAX®1074-Based mixed matrix membranes to be used in humidifiers in proton exchange membrane fuel cells, *E-Polymers* 20 (1) (2020) 171–184, <https://doi.org/10.1515/EPOLY-2020-0022/MACHINEREADABLECITATION/RIS>.
- [24] N. Azizi, T. Mohammadi, R.M. Behbahani, Synthesis of a new nanocomposite membrane (PEBAX-1074/PEG-400/TiO₂) in order to separate CO₂ from CH₄, *J. Nat. Gas Sci. Eng.* 37 (2017) 39–51, <https://doi.org/10.1016/J.JNGSE.2016.11.038>.
- [25] W. Li, Z. Chang, L. Lin, X. Xu, Effect of montmorillonite on PEBAX® 1074-based mixed matrix membranes to be used in humidifiers in proton exchange membrane fuel cells, *E-Polymers* 20 (1) (2020) 171–184, <https://doi.org/10.1515/EPOLY-2020-0022>.
- [26] A. Atash Jameh, T. Mohammadi, O. Bakhtiari, Preparation of PEBAX-1074/modified ZIF-8 nanoparticles mixed matrix membranes for CO₂ removal from natural gas, *Sep. Purif. Technol.* 231 (2020), 115900, <https://doi.org/10.1016/J.SEPPUR.2019.115900>.
- [27] M. Djabourov, J. Leblond, P. Papon, Gelation of aqueous gelatin solutions. I. Structural investigation, *J. Phys.* 49 (2) (1988) 319–332, <https://doi.org/10.1051/jphys:01988004902031900i>.
- [28] V.I. Bondar, B.D. Freeman, I. Pinnau, Gas transport properties of poly(ether-b-amide) segmented block copolymers, *J. Polym. Sci., Part B: Polym. Phys.* 38 (15) (2000) 2051–2062, [https://doi.org/10.1002/1099-0488\(20000801\)38:15<2051::AID-POLB100>3.0.CO;2-D](https://doi.org/10.1002/1099-0488(20000801)38:15<2051::AID-POLB100>3.0.CO;2-D).
- [29] N-METHYL-2-PYRROLIDONE | CAMEO chemicals | NOAA. <https://cameochemicals.noaa.gov/chemical/8857>. (Accessed 22 June 2022).
- [30] B.E. Poling, J.M. Prausnitz, J.P. O'connell, N. York, C. San, F. Lisbon, L. Madrid, M. City, M.N. Delhi, S. Juan, THE PROPERTIES OF GASES AND LIQUIDS, fifth ed., McGRAW-HILL, 2001.
- [31] R.W. Baker, Membrane Technology and Applications, second ed., John Wiley & Sons, Inc., 2007.
- [32] M. Mulder, Basic Principles of Membrane Technology, 1991, https://doi.org/10.1524/zpch.1998.203.part_1_2.263.
- [33] L.M. Robeson, The upper bound revisited, *J. Membr. Sci.* 320 (1–2) (2008) 390–400, <https://doi.org/10.1016/J.MEMSCI.2008.04.030>.
- [34] B.W. Rowe, L.M. Robeson, B.D. Freeman, D.R. Paul, Influence of temperature on the upper bound: theoretical considerations and comparison with experimental results, *J. Membr. Sci.* 360 (1–2) (2010) 58–69, <https://doi.org/10.1016/J.MEMSCI.2010.04.047>.
- [35] K. Xie, Q. Fu, G.G. Qiao, P.A. Webley, Recent progress on fabrication methods of polymeric thin film gas separation membranes for CO₂ capture, *J. Membr. Sci.* (2019), <https://doi.org/10.1016/j.memsci.2018.10.049>.
- [36] V.I. Bondar, B.D. Freeman, I. Pinnau, Gas sorption and characterization of poly(ether-b-amide) segmented block copolymers, *J. Polym. Sci., Part B: Polym. Phys.* (1999), [https://doi.org/10.1002/\(sici\)1099-0488\(19990901\)37:17<2463::aid-polb18>3.3.co;2-8](https://doi.org/10.1002/(sici)1099-0488(19990901)37:17<2463::aid-polb18>3.3.co;2-8).
- [37] J. Marcq, T.N. Quang, D. Langevin, B. Brule, Abatement of CO₂ emissions by means of membranes - characterization of industrial Pebax™ films, *Environ. Protect. Eng.* (2005).
- [38] H. Sijbesma, K. Nijmeijer, R. van Marwijk, R. Heijboer, J. Potreck, M. Wessling, Flue gas dehydration using polymer membranes, *J. Membr. Sci.* (2008), <https://doi.org/10.1016/j.memsci.2008.01.024>.